

## INFLUENCE OF INSPECTION RAILS ON AERODYNAMICS OF A LONG-SPAN BRIDGE DECK: A NUMERICAL STUDY

Md. N. Haque\*<sup>1</sup> and Hiroshi Katsuchi<sup>2</sup>

<sup>1</sup> Lecturer, Dept. of Civil Engineering, Chittagong University of Engineering and Technology, Bangladesh, e-mail: [naimulce@gmail.com](mailto:naimulce@gmail.com)

<sup>2</sup> Professor, Dept. of Civil Engineering, Yokohama National University, Japan, e-mail: [katsuchi@ynu.ac.jp](mailto:katsuchi@ynu.ac.jp)

### ABSTRACT

*Aerodynamics of the long-span bridge deck with section details should be well investigated to improve understanding and ensure the stability of the bridge deck against wind. In this study, the influence of inspection rails on aerodynamics of a long-span bridge deck was investigated by two-dimensional Computational Fluid Dynamics (CFD) using Unsteady RANS (URANS) turbulence model. The behaviour of the static force coefficients and after-body vortex shedding characteristics were analysed in detailed. The flow field was explored elaborately by means of surface pressure and velocity distributions. Along with the presence of inspection rails, the locations of inspection rails on aerodynamic characteristics were also explored. It was found that the presence of the inspection rails deteriorates the aerodynamic characteristics, yet a comparatively better aerodynamic performance can be obtained by attaching them at an appropriate location.*

**Keywords:** *Inspection rails; Bridge deck; Aerodynamics and CFD*

### 1. INTRODUCTION

Long-span Bridge decks often suffer from aeroelastic problems. Engineers should have improved understanding about the aerodynamics of the long-span bridge deck to avoid wind-induced instabilities. A long-span bridge deck has various additional parts such as the handrails, side curb, median curb, traffic barriers, central stabilizers and inspection rails etc. However, their influence on aerodynamic responses is not fully understood yet. Even though, these addition parts are quite small as compared to the size of the bridge deck, their presence may alter the aerodynamics of the bridge deck and jeopardize the bridge deck stability as aerodynamic response is a quite sensitive quantity.

Previously, the qualitative influence of traffic barriers on aerodynamic responses was shown by Bienkiewicz (1987). Then, Scanlan, Jones, Sarkar & Singh (1995) conducted wind tunnel investigation and showed the dependence of flutter on small section details such as handrails. Nagao, Utsunomiya, Yoshioka, Ikeuchi & Kobayashi (1997) studied the influence of handrails on vortex-induced vibration and found that the presence of handrail enhances the vertical vortex-induced vibration, yet weakens the torsional vortex-induced vibration. After that, Bruno and Mancini (2002) carried out CFD analysis for the great-belt bridge deck to show the influence of handrails on the steady state response and the flow field. Sarwar, Ishihara, Shimada, Yamasaki & Ikeda (2008) analysed the effects of handrails and inspection rails on the force coefficients and flutter derivatives by means of CFD simulation. However, previous investigations mainly focused on the handrails without taking into care of the influence of inspection rails in details, yet the inspection rails are one of the most common parts of the long-span bridge deck used to place the overhead and gantry crane for construction and maintenance purpose. Moreover, previous investigation was focused primarily on the quantitative response only without detailed investigation of the flow field to understand the flow mechanism. In addition, these kind of additional parts are small in size, their influence on flow fields is mainly the interference phenomena with the bridge deck. Therefore, influence on aerodynamic response and the flow mechanism will differ depending on the shape of the bridge deck. Further, inspection rails are being attached at various locations at the bottom deck surface without knowing the influence of inspection rails position on aerodynamic responses. Still the appropriate location of attaching inspection rails on the bridge deck is not known to obtain better aerodynamic performance.

In the present study the influence and location of inspection rails on aerodynamics of a single box hexagonal shaped bridge deck was investigated as shown in Figure 1(a). The hexagonal shaped bridge deck has become a popular shape in Japan and recently a number of long-span bridge decks such as Takeshima Bridge, Shintenmom Bridge, Oshima Bridge and Kesenuma Bridge etc. in Japan have adopted this type of shape. For

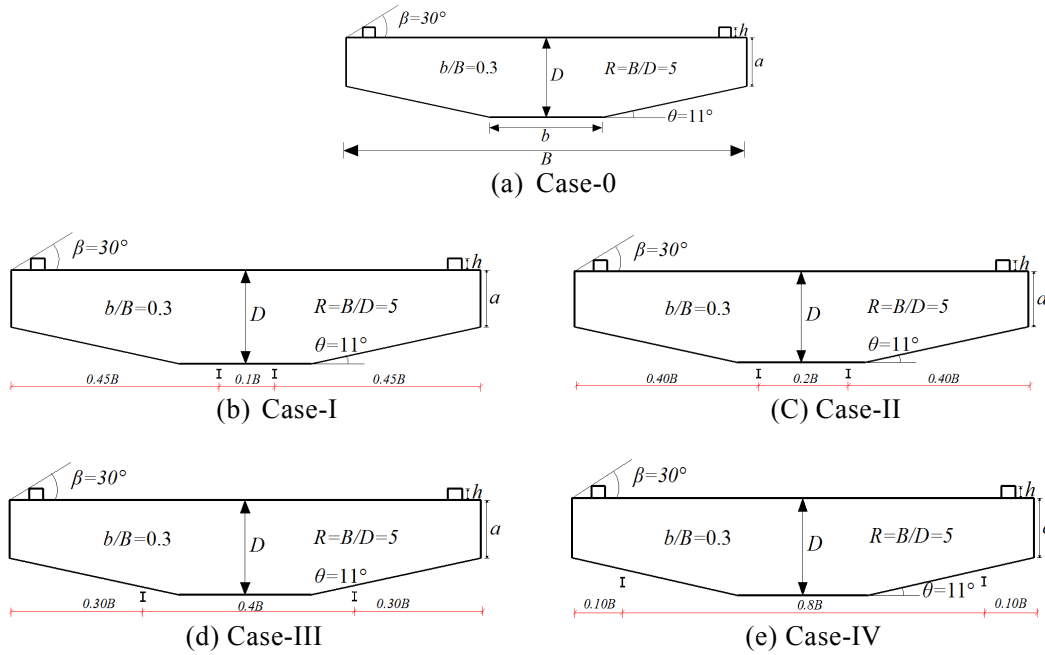


Figure 1: Detailed configuration of the bridge deck and various locations of inspection rails considered in the present study: (a) Basic deck section and (b~e) Deck section with inspection rail

this kind of bridge deck, the top deck flow is controlled by the side curb is known as Separation Interference Method (SIM) proposed by Kubo, Yoshida, Tuji, Kimura & Kato (2007) and the bottom deck flow is controlled by the bottom plate slope ( $\theta$ ). Four different locations of inspection rails were explored as shown in Figure 1. First, the effects of inspection rails on steady state force coefficients were observed. Then, the pressure and velocity fields were explored in detailed to understand the responses and the flow fields. The wake characteristics were also analysed elaborately. Finally, based on observation and understanding recommendations were made regarding the placement position of inspection rails at the bridge deck.

## 2. NUMERICAL PROCEDURE

The unsteady Reynolds-Averaged Navier-Stokes (URANS) equations were used to model the flow around the bridge deck. Flow was assumed to be two dimensional and incompressible in nature. The governing equations were as follows;

$$\frac{\partial \bar{U}_i}{\partial x_i} = 0 \quad (1)$$

$$\frac{\partial \bar{U}_i}{\partial t} + \bar{U}_j \frac{\partial \bar{U}_i}{\partial x_j} = -\frac{1}{\rho} \frac{\partial \bar{P}}{\partial x_i} + \frac{\partial}{\partial x_j} \left[ \nu \left( \frac{\partial \bar{U}_i}{\partial x_j} + \frac{\partial \bar{U}_j}{\partial x_i} \right) - (\overline{u'_i u'_j}) \right] \quad (2)$$

where,  $\bar{U}_i$  and  $x_i$  are the averaged velocity and position vectors respectively,  $t$  is the time,  $\bar{P}$  is the averaged pressure,  $\rho$  is the air density,  $\nu$  is the fluid viscosity. Due to time averaging process, the new variable  $\overline{u'_i u'_j}$  appeared, which is known as Reynolds stress. It needs modelling to close the equation, which is known as turbulence modelling. In this work turbulence modelling was attained by  $k-\omega$ -SST, a two equations turbulence model (Menter 1994). This model has combined the best of the  $k-\epsilon$  and  $k-\omega$  models. Further details of the model can be found in Menter (1994) and Menter, Kuntz & Langtry (2003). The Convective and diffusive terms in the governing equation were discretized with second order accurate central differencing schemes. For time integration second order accurate backward differentiation formulae method was utilized. PISO (Pressure implicit with splitting of operator) algorithm was utilized to solve those discretized equations. An open source code OpenFOAM was used.

A two dimensional domain with 48D in the lengthwise direction and 25D in the vertical direction, where  $D$  is the height of the bridge deck section was used to conduct the simulation. The object was placed at 18D downstream of the inlet. The outlet boundary was placed at 25D downstream of the object and height of the domain was 25D. The height of the domain was justified in Haque, Katsuchi, Yamada & Nishio (2015a). At the outlet, pressure boundary condition, at the top and bottom of the domain, slip boundary condition and at the body, non-slip boundary condition was implemented. The domain was discretized spatially by a non-uniform structured grid and the cell size was varied gradually with a geometric progression of 1.05 in all directions based on previously proposed strategy (Haque et al. 2015a). The first cell height away from the body was selected such a way that the normalized wall distance ( $y^+$ ) remains a value near about 5. Further details of the setup and validation of the study can be found in Haque et al. (2014); (2015a) and (2015b).

### 3. AERODYNAMIC BEHAVIOR OF THE BRIDGE DECK

Influence of inspection rails on aerodynamic characteristics of the bridge decks was investigated for a hexagonal shaped bridge deck as shown in Figure 1(a). The bridge deck had a side ratio ( $R$ ) of 5 and a width ratio ( $W$ ) of 0.3. The curb angle ( $\beta$ ) and height ( $h/D$ ) was set to  $30^\circ$  and 0.115, respectively. Four different locations of inspection rails were considered and named sequentially as summarized in Figure 1(b) to Figure 1(e). There was a normalized (normalized with the depth of the deck,  $D$ ) gap of 0.07 between the deck and the inspection rails. All the simulations were conducted at a Reynolds number ( $Re$ ) of  $1.2 \times 10^4$ .

#### 3.1 Aerodynamic Coefficients

The important aerodynamic coefficients such as the drag ( $C_D$ ), lift ( $C_L$ ) and moment ( $C_M$ ) were calculated. The drag ( $C_D$ ) was normalized with the depth ( $D$ ) of the bridge deck while the lift ( $C_L$ ) and moment ( $C_M$ ) were normalized with the width ( $B$ ) of the bridge deck. Figure 2 depicts the time history of the force coefficients. The presence of inspection rails alter the responses noticeably and depending on the location of inspection rails the response also varies. At the very first sight, it can be realized that the Case-IV has the closest responses to the basic section (Case-0). Table 1 summarizes the statistical parameters of the aerodynamic coefficients. Table 1 reflects the general observation we made earlier. All the mean value of the force and moment coefficients deteriorates due to addition of inspection rails to the bridge deck. As the inspection rails are attached, the drag and moment values increase and the lift value becomes positive. However, the Case-IV has the least responses among the four considered positions. In contrary to the mean value, the rms fluctuation and the strouhal number ( $S_r$ ) show different trends in the results. As the inspection rails are attached to the bridge deck, the fluctuation and strouhal number ( $S_r$ ) decrease. To enhance the understanding of the obtained results the flow fields are analysed in the next section.

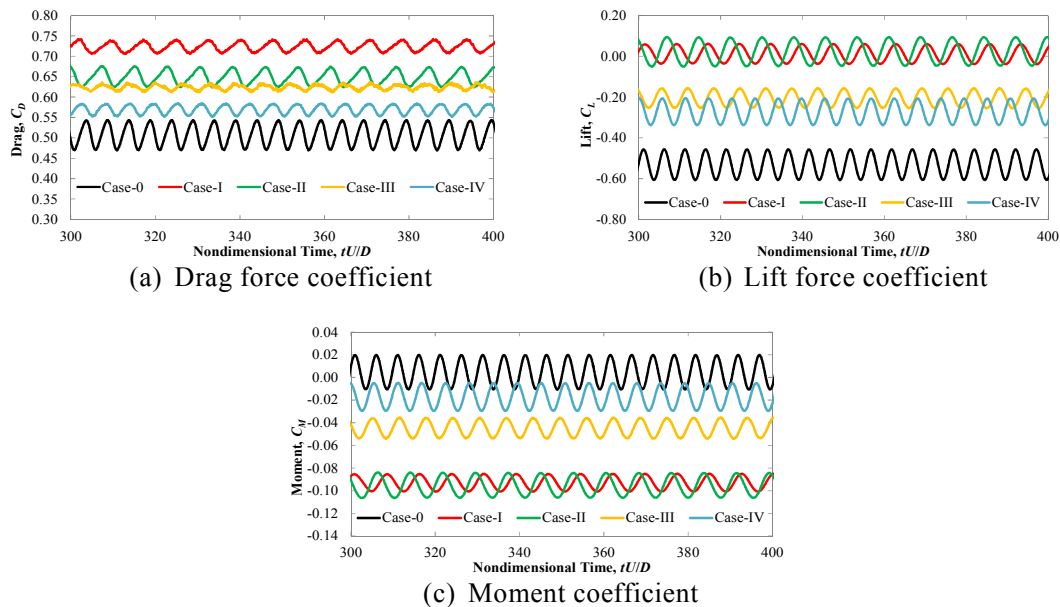


Figure 2: Time history of important force and moment coefficients

Table 1: Mean and rms value of aerodynamic coefficients

| Case No. | Mean drag ( $C_D$ ) | Mean Lift ( $C_L$ ) | Mean Moment ( $C_M$ ) | rms Lift ( $C_L'$ ) | rms moment ( $C_M'$ ) | Strouhal number ( $S_t$ ) |
|----------|---------------------|---------------------|-----------------------|---------------------|-----------------------|---------------------------|
| 0        | 0.508               | -0.532              | 0.005                 | 0.053               | 0.011                 | 0.198                     |
| I        | 0.724               | 0.011               | -0.093                | 0.034               | 0.006                 | 0.132                     |
| II       | 0.649               | 0.023               | -0.095                | 0.049               | 0.008                 | 0.129                     |
| III      | 0.624               | -0.206              | -0.045                | 0.034               | 0.006                 | 0.158                     |
| IV       | 0.569               | -0.273              | -0.017                | 0.046               | 0.009                 | 0.177                     |

3.2 Flow Field Analysis

The mean surface pressure distributions around the considered cases are presented in Figure 3. The mean pressure distribution doesn't show any distinct trend in the results. The variation of the location of inspection rails mainly affects the bottom surface leading edge pressure distribution. In case of Case-II and Case-III, there is minimum suction in the leading edge bottom deck surface; hence the lift value becomes positive in those cases. For the same reason, those two cases have the highest negative moment values.

The rms value of pressure distributions are plotted in Figure 4. The rms pressure is mainly affected at the trailing edge side. Even though the inspection rails were attached at the bottom surface, the top surface pressures were also affected due to the variation of inspection rails location. The trailing edge vortices are the main cause of this kind of large rms value at the trailing edge side (Haque et al. 2015b).

The time averaged velocity distributions are compared in Figure 5. As can be seen the flow behaviour alters significantly due to presence of the inspection rails. Both the leading edge and bottom side separation enhances when the inspection rails are attached to the bridge deck. When the distance between the inspection rails are small (Figures 5(b) and (c)), the leeward side inspection rail remains in the wake of the windward side

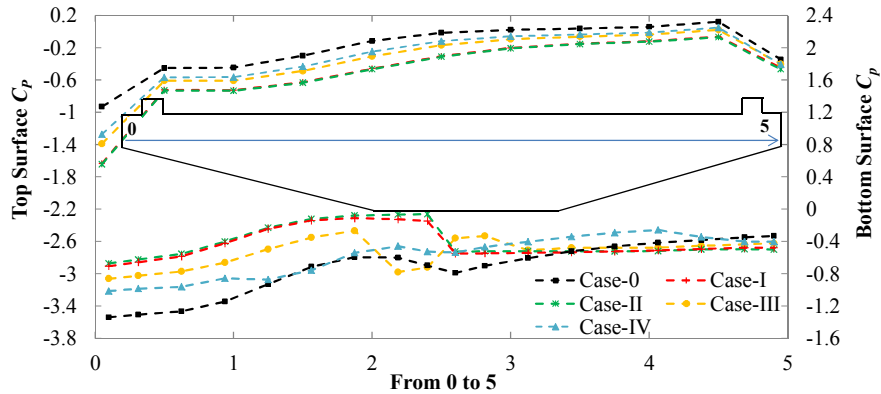


Figure 3: Influence of inspection rails on mean pressure distribution around the bridge deck

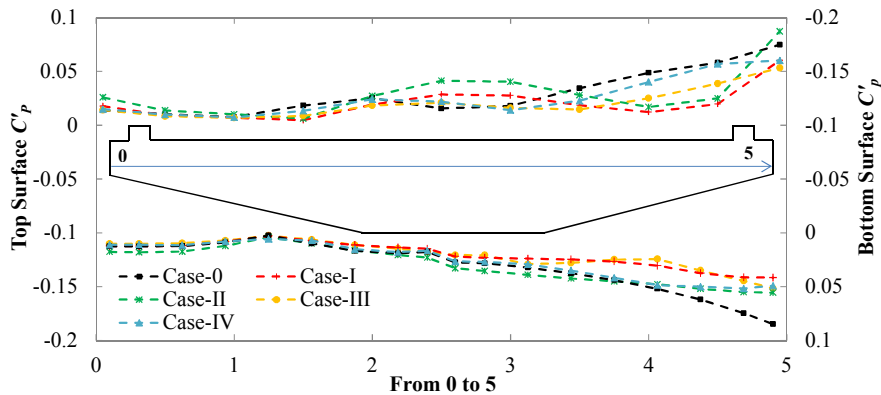


Figure 4: Influence of inspection rails on rms pressure distribution around the bridge deck

inspection rail. However, as long as the distance between the inspection rails increases (Figures 5(d) and (e)), the flow again obstructed by the leeward side inspection rails. When the inspection rails are attached at the bottom horizontal plate (Figures 5(b) and (c)), being obstructed by the windward side inspection rail, the flow doesn't reattach at the trailing edge side of the bridge deck. Therefore, the synchronization between the after-body vortices decreases and decreases the rms fluctuations. However, when the inspection rails are attached at the inclined plate of the bridge (Figures 5(d) and 5(e)), the flow reattaches again after obstructed by the windward side inspection rails and the vortex forms at the side of the bridge deck. As a result the synchronization among the vortices increases again and the rms fluctuation increases. Further, the wake size of the bridge deck decreases in case of Case-III and Case-IV. The wake velocity distributions are plotted in Figure 6. The general observation about the wake is also reflected in Figure 6. When the inspection rails are attached at the inclined plate, the wake of the bridge deck decreases and becomes similar to the distribution of the basic section. In a consequence, the drag of the bridge deck decreases in case of Case-IV.

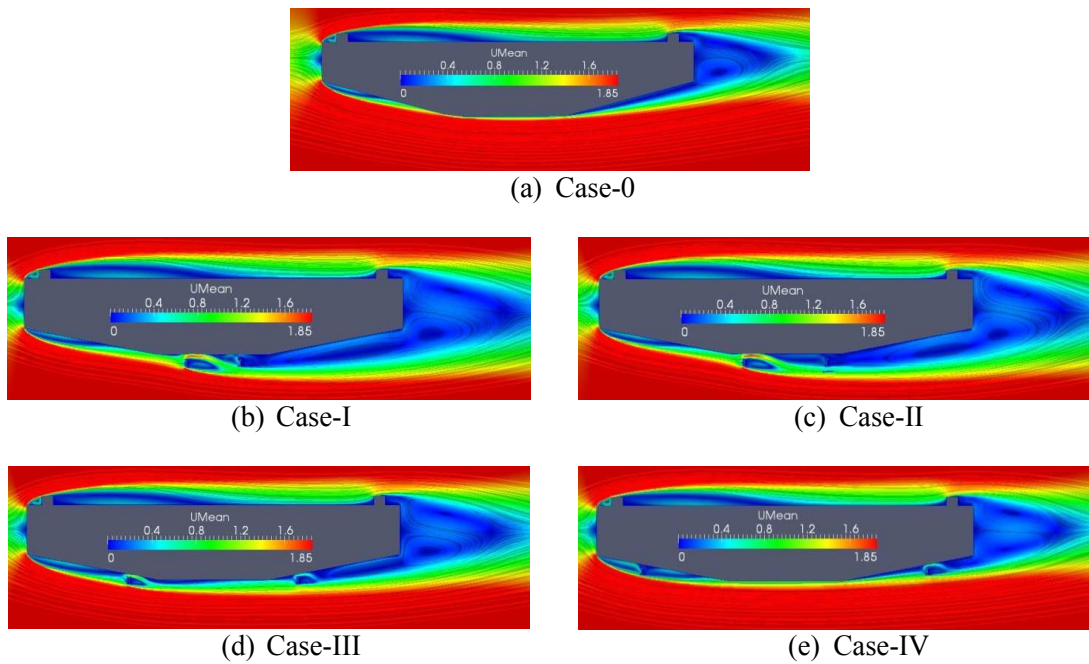


Figure 5: Influence of inspection rails on the flow field around the bridge deck

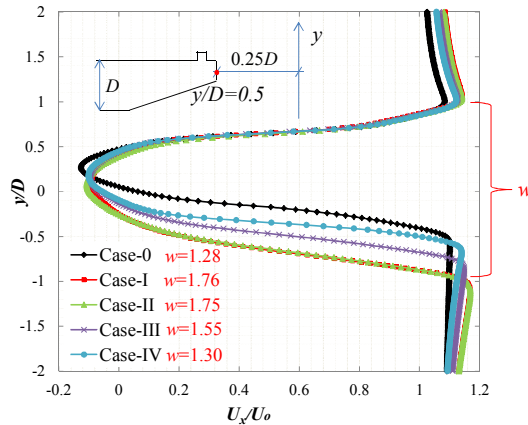


Figure 6: Influence of inspection rails on the wake characteristics of the bridge deck

#### 4. CONCLUSIONS

In the present study, the effects of inspection rails and its location on aerodynamic response of a hexagonal shaped bridge deck were analysed. The pressure and velocity distributions were taken into consideration to understand the flow field and to explain the static responses. It was found that the presence of inspection rails increases and deteriorates the aerodynamic responses. Further, depending on the locations of the inspection rails the responses alters too. However, the aerodynamic responses can be optimized by attaching the inspection rails at some particular locations. When the inspection rails are attached at the inclined bottom plate surface of the bridge deck, the flow remains attached to the bridge deck surface and possess smaller wake and exhibits better aerodynamic characteristics. Therefore, for this kind of hexagonal shaped bridge deck the inspection rails can be attached at the inclined bottom plate of the bridge deck. However, depending on the bridge deck shape the flow mechanism due to presence of inspection rails may alter. Further detailed and elaborate investigation should be carried out before attaching inspection rails to the bridge deck other than the considered shape.

#### REFERENCES

- Bienkiewicz, B. (1987). Wind tunnel study of geometry modification on aerodynamics of a cable-stayed bridge deck. *Journal of Wind Engineering and Industrial Aerodynamics*, 26, 325–339.
- Bruno, L. & Mancini, G. (2002). Importance of deck details in bridge aerodynamics. *Structural Engineering International*, 12(4), 289-294.
- Haque, M.N., Katsuchi, H., Yamada, H. & Nishio, M. (2014). *Investigation of Bridge Deck Shaping Effects on Aerodynamic Response by RANS Simulation*. Proceedings of 6th International Symposium on Computational Wind Engineering (CD-ROM), June 8-12, Hamburg University, Hamburg, Germany.
- Haque, M.N., Katsuchi, H., Yamada, H. & Nishio, M. (2015a). Strategy to develop efficient grid system for flow analysis around two-dimensional bluff bodies. *KSCE Journal of Civil Engineering*. 10.1007/s12205-015-0696-2
- Haque, M.N., Katsuchi, H., Yamada, H. & Nishio, M. (2015b). A numerical study on aerodynamics of a pentagonal shaped cable-supported bridge deck. *Journal of Structural Engineering (JSCE)*, 61A, 375-387.
- Kubo, Y., Yoshida, K., Tuji, E., Kimura, K. & Kato, K. (2007). *Development of aerodynamically stable bridge girder cross section for long span bridges*. Proceedings of 12th International Conference on Wind Engineering, 1-6 July, Cairns, Australia, 239-246.
- Menter, F.R. (1994). Two-equation eddy-viscosity turbulence models for engineering application, *AIAA Journal*, 32, 1589-1605.
- Menter, F.R., Kuntz, M. & Langtry, R. (2003). Ten years of industrial experience with the SST turbulence model. *Turbulence, Heat and Mass Transfer*, 4, 625–632.
- Nagao, F., Utsunomiya, H., Yoshioka, E., Ikeuchi, A. & Kobayashi, H. (1997). Effects of handrails on separated shear flow and vortex-induced oscillation. *Journal of Wind Engineering and Industrial Aerodynamics*, 69-71, 819-827.
- Sarwar, M.W., Ishihara, T., Shimada, K., Yamasaki, Y. & Ikeda, T. (2008). Prediction of aerodynamic characteristics of a box girder bridge section using the LES turbulence model. *Journal of Wind Engineering and Industrial Aerodynamics*, 96, 1895-1911.
- Scanlan, R.H., Jones, N.P., Sarkar, P.P. & Singh, L. (1995). The effect of section model on aeroelastic parameters, *Journal of Wind Engineering and Industrial Aerodynamics*, 54-55, 45–53.